

A Deep Learning Classifier Using Sliding Patches for Detection of Mammographical Findings

Diego Mellado, Marvin Querales, Julio Sotelo, Eduardo Godoy, Fabian Pardo, Scarlett Lever, Stéren Chabert, Rodrigo Salas

Doctorado en Ciencias e Ingeniería para la Salud, Universidad de Valparaíso

November 16th, 2023



This work was funded by:

- National Agency for Research and Development (ANID) / Scholarship program / *Becas Doctorado Nacional 2022 - 21221429*
- Millenium Science Initiative Program ICN2021_004
- ANID FONDEF IDEA I+D ID20i10332 "*Artificial Intelligence System for Support in Diagnosis and Priorization of Mammographic Exams*"
- ANID FONDECYT Research Grant 1221938



Millennium Institute
for Intelligent
Healthcare Engineering



- Worldwide, has an average mortality rate of 13.6 per 100 000 women in 2020 ¹
- In Chile, has an average mortality rate of 11.8 per 100 000 women, as of 2018 ²
- Early diagnosis and survival rate in Chile has increased due to the implementation of screening programs ³

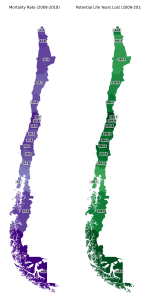


Figure: Mortality rate and number of potential lost years of life due to breast cancer in Chilean Women (2009-2018)

¹Breast Cancer Statistics | World Cancer Research Fund International. WCRF International. URL: <https://www.wcrf.org/cancer-trends/breast-cancer-statistics/> (visited on 11/09/2023)

²Ministerio de Salud. Informe de Vigilancia de Cáncer. Análisis de Mortalidad Prematura y AVPP Por Cáncer. Década 2009-2018. Chile: Departamento de Epidemiología, 2021. URL: <https://www.minsal.cl/wp-content/uploads/2022/01/Informe-Mortalidad-Prematura-y-AVPP-por-C%C3%A1ncer-2009-2018.pdf> (visited on 11/09/2023)

³César del SM Castillo, M. Elena C. Cabrera, Lea Derio P., et al. "Resultados Del Tratamiento Del Cáncer de Mama, Programa Nacional de Cáncer Del Adulto". In: Revista médica de Chile 145.12 (Dec. 2017), pp. 1507-1513. ISSN: 0034-9887. DOI: 10.4067/s0034-98872017001201507. URL: https://scielo.conicyt.cl/scielo.php?script=sci_abstract&pid=S0034-98872017001201507&lng=es&nrm=iso&tlang=en (visited on 04/21/2021)

- Machine Learning and Deep Learning models have been implemented for the detection of breast cancer in mammograms.⁴
- Current Challenges:
 - Detection of breast lesion location in mammograms⁵
 - Visualisation tools for interpretation of prediction models.
 - Breast Density Estimation
 - Breast image classification beyond malignity.

⁴ Alejandro Rodríguez-Ruiz, Elizabeth Krupinski, Jan-Jurre Mordang, et al. "Detection of Breast Cancer with Mammography: Effect of an Artificial Intelligence Support System". In: *Radiology* 290.2 (Nov. 20, 2018), pp. 305–314. ISSN: 0033-8419. DOI: 10.1148/radiol.2018181371. URL: <https://pubs.rsna.org/doi/10.1148/radiol.2018181371> (visited on 05/12/2021)

⁵ O. Díaz, A. Rodríguez-Ruiz, A. Gubern-Mérida, et al. "¿Son los sistemas de inteligencia artificial una herramienta útil para los programas de cribado de cáncer de mama?" In: *Radiología* 63.3 (May 2021), pp. 236–244. ISSN: 00338338. DOI: 10.1016/j.rx.2020.11.006. URL: <https://linkinghub.elsevier.com/retrieve/pii/S0033833820301752> (visited on 03/30/2023)

Ertosun and Rubin proposed a Deep Learning model for visual search in mammograms using a regional probabilistic approach.⁶

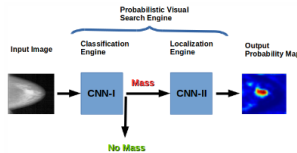


Figure: Probabilistic Visual Search Engine proposed by Ertosun and Rubin

⁶ Mehmet Gunhan Ertosun and Daniel L. Rubin. "Probabilistic Visual Search for Masses within Mammography Images Using Deep Learning". In: *2015 IEEE International Conference on Bioinformatics and Biomedicine (BIBM)*. 2015 IEEE International Conference on Bioinformatics and Biomedicine (BIBM). Washington, DC, USA: IEEE, Nov. 2015, pp. 1310–1315. ISBN: 978-1-4673-6799-8. doi: 10.1109/BIBM.2015.7359868. URL: <http://ieeexplore.ieee.org/document/7359868/> (visited on 11/09/2023)

⁷ Steven J. Frank. "A Deep Learning Architecture with an Object-Detection Algorithm and a Convolutional Neural Network for Breast Mass Detection and Visualization". In: *Healthcare Analytics* 3 (Nov. 1, 2023), p. 100186. ISSN: 2772-4425. doi: 10.1016/j.health.2023.100186. URL: <https://doi.org/10.1016/j.health.2023.100186>

Ertosun and Rubin proposed a Deep Learning model for visual search in mammograms using a regional probabilistic approach.⁶

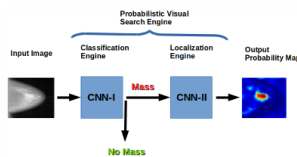


Figure: Probabilistic Visual Search Engine proposed by Ertosun and Rubin

Frank proposed using YOLO V5 for detection of breast lesions, combined with EfficientNet for classification of masses and microcalcifications.⁷

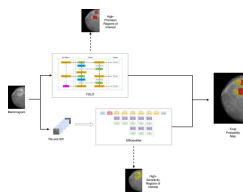


Figure: Combined detection model and classifier for breast cancer proposed by Frank

⁶ Mehmet Gunhan Ertosun and Daniel L. Rubin. "Probabilistic Visual Search for Masses within Mammography Images Using Deep Learning". In: *2015 IEEE International Conference on Bioinformatics and Biomedicine (BIBM)*. 2015 IEEE International Conference on Bioinformatics and Biomedicine (BIBM). Washington, DC, USA: IEEE, Nov. 2015, pp. 1310–1315. ISBN: 978-1-4673-6799-8. doi: 10.1109/BIBM.2015.7359868. URL: <http://ieeexplore.ieee.org/document/7359868/> (visited on 11/09/2023)

⁷ Steven J. Frank. "A Deep Learning Architecture with an Object-Detection Algorithm and a Convolutional Neural Network for Breast Mass Detection and Visualization". In: *Healthcare Analytics* 3 (Nov. 1, 2023), p. 100186. ISSN: 2772-4425. doi: 10.1016/j.health.2023.100186. URL: <https://doi.org/10.1016/j.health.2023.100186>

Ertosun and Rubin proposed a Deep Learning model for visual search in mammograms using a regional probabilistic approach.⁶

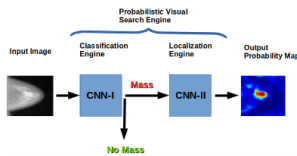


Figure: Probabilistic Visual Search Engine proposed by Ertosun and Rubin

Frank proposed using YOLO V5 for detection of breast lesions, combined with EfficientNet for classification of masses and microcalcifications.⁷

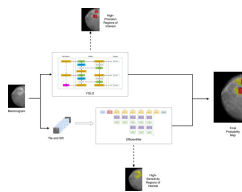


Figure: Combined detection model and classifier for breast cancer proposed by Frank

Yi, Sawyer, Cohn III, et al. proposed a model for visualization of shared features between views of the breast for classification of benign and malignant breast tumours.⁸

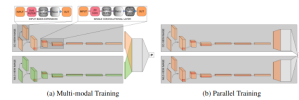


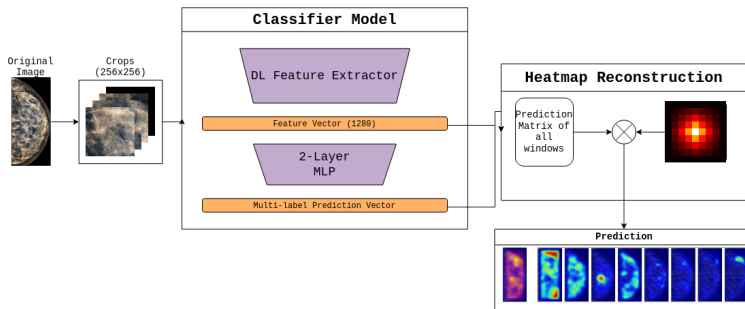
Figure: Multimodal architecture proposed by Yi, Sawyer, Cohn III, et al. for visualization of shared features between views of the breast.

⁶ Mehmet Gunhan Ertosun and Daniel L. Rubin. "Probabilistic Visual Search for Masses within Mammography Images Using Deep Learning". In: *2015 IEEE International Conference on Bioinformatics and Biomedicine (BIBM)*. 2015 IEEE International Conference on Bioinformatics and Biomedicine (BIBM). Washington, DC, USA: IEEE, Nov. 2015, pp. 1310–1315. ISBN: 978-1-4673-6799-8. doi: 10.1109/BIBM.2015.7359868. URL: <http://ieeexplore.ieee.org/document/7359868/> (visited on 11/09/2023)

⁷ Steven J. Frank. "A Deep Learning Architecture with an Object-Detection Algorithm and a Convolutional Neural Network for Breast Mass Detection and Visualization". In: *Healthcare Analytics* 3 (Nov. 1, 2023), p. 100186. ISSN: 2772-4425. doi: 10.1016/j.health.2023.100186. URL: <https://doi.org/10.1016/j.health.2023.100186>

Our study proposes a Deep Learning Classifier trained on cropped segments of mammograms for multi-label classification of pathological findings.

General Inspection of the complete image using local patches to identify the probability of the presence of a pathological finding.



- **Vindr-mammo Dataset⁹**
- 5000 digital mammogram examinations containing for each view:
 - BIRADS
 - Breast density
 - Bounding box of each finding present on the image
- 10 classes of pathological findings.
- Bounding boxes can have multiple labels.

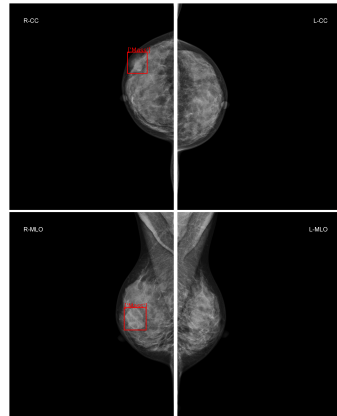


Figure: Example of a mammogram from the Vindr-mammo dataset.

⁹Hieu Huy Pham, Hieu Nguyen Trung, and Ha Quy Nguyen. VinDr-Mammo: A Large-Scale Benchmark Dataset for Computer-Aided Detection and Diagnosis in Full-Field Digital Mammography. Version 1.0.0. PhysioNet. DOI: 10.13026/BR2V-7517. URL: <https://physionet.org/content/vindr-mammo/1.0.0/> (visited on 11/08/2022)

Table: Findings statistics of Vindr-Mammo Dataset

Finding	Training	Test	Total
Mass	989	237	1226
Suspicious Calcification	428	115	543
Asymmetries (Global, Focal, etc.)	313	79	392
Architectural Distortion	95	24	119
Skin Thickening	45	12	57
Retraction (Skin or Nipple)	45	10	55
Suspicious Lymph Node	46	7	37

- Each DICOM Image is normalised to a range of [0, 1]
- Apply CLAHE algorithm¹⁰ for histogram equalization at 2 different scales
- Fuse the equalized images with the original, channel-wise
- Image is cropped to the bounding box of the breast using Otsu's thresholding.

¹⁰ S.M. Pizer, R.E. Johnston, J.P. Erickson, et al. "Contrast-Limited Adaptive Histogram Equalization: Speed and Effectiveness". In: *[1990] Proceedings of the First Conference on Visualization in Biomedical Computing*. [1990] Proceedings of the First Conference on Visualization in Biomedical Computing. May 1990, pp. 337–345. doi: 10.1109/VBC.1990.109340. URL: <https://ieeexplore.ieee.org/document/109340> (visited on 10/03/2023)

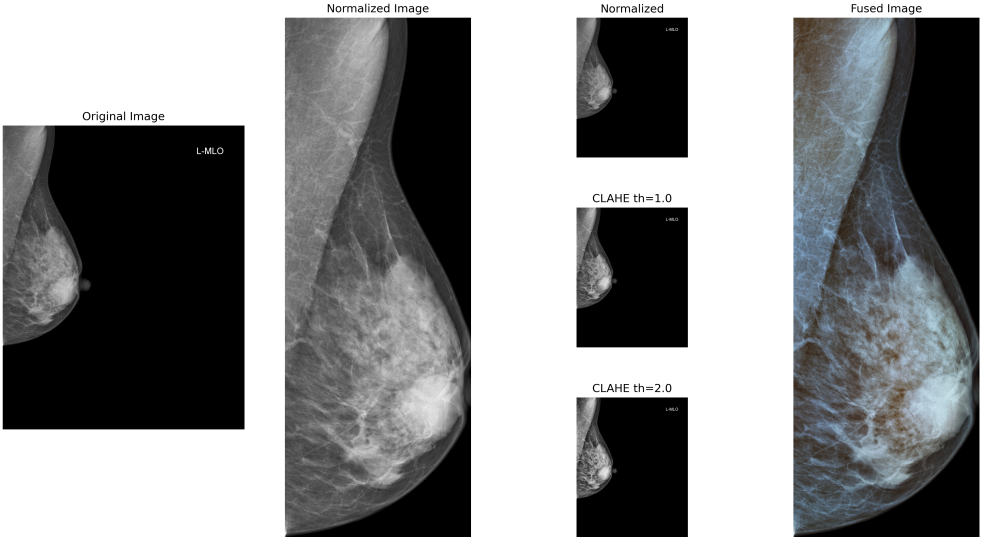


Figure: Image processing pipeline

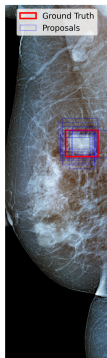
We evaluated the following architectures as a backbone:

- ResNet50 [6]
- EfficientNetV2 [15]
- DenseNet121 [8]
- Swin Transformer [9]
- MobileNet [7]
- VGG19 [14]
- Dropout of 0.5 after the backbone.
- Classifier Layer using a 2-layer MLP with 512 hidden units and ReLU activation.
- Output layer with sigmoid activation.

- We use the backbone of the selected architecture as a feature extractor.
- The output of the backbone is flattened and fed to the classifier.
- The classifier is trained using the cropped images.

- For each finding present on an image, we sampled a random area of the finding.
- Area and aspect ratio randomly sampled from an Uniform distribution.
 - Area: [.05, 5.] of the finding bounding box area.
 - Aspect ratio: [0.33, 1.66] of the finding bounding box aspect ratio.
 - The bounding box center is uniform sampled from 50 px around the original center.
- For normal images (*No Finding*), we sample a random area of the breast, with similar sampling parameters.
- Sampled image is resized to 256×256 pixels.
- Image augmentation:** Contrast, brightness, saturation, flip and rotation are randomly modified.

Original Image



Proposals

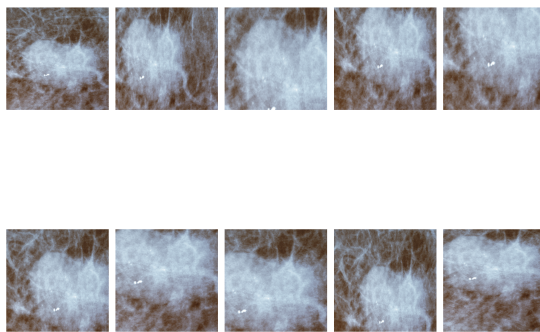


Figure: Example of sampling of ten positive proposals from a finding.

- Focal Loss Function

$$\mathcal{L}_{\text{Focal}} = -(1 - p_t)^\gamma \log (p_t)$$

- Adam Optimizer with a starting learning rate of 1×10^{-4}
- Reduce on plateau with a patience of 5 epochs and a factor of 0.1
- Weighted sampling of the dataset, in order to reduce imbalance.

- Segmentation of the complete image into a set of overlapping windows of size 256×256 pixels and stride of 32 px.
- Reconstruction of prediction heatmap from the overlapping windows.
- Feature visualization by weighted sum of feature maps, based on most important features. Using a Random Forest Classifier trained on the features extracted from the training set.
- Random Forest Classifier achieves similar results as the MLP classifier, used only to identify the most important features.

Table: F1 Score for Pathological findings classification task with Vindr, comparing different Deep Learning Models.

	N	DenseNet	EfficientNet	ResNet50	SwinTransformer	VGG19	MobileNet
Mass	237	0.783	0.815	0.742	0.770	0.756	0.708
Suspicious Calcification	115	0.847	0.865	0.860	0.828	0.873	0.828
Assymetries	79	0.306	0.295	0.200	0.310	0.204	0.324
Suspicious Lymph Node	11	0.667	0.500	0.737	0.370	0.400	0.476
Weighted Average	442	0.712	0.727	0.675	0.693	0.679	0.665

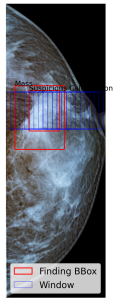
EfficientNet has the best overall performance, with an F1 score of 0.727. We chose this model as the backbone for our classifier.

Table: Metrics of pathological findings classification task using Vindr

	Accuracy	Precision	Recall	F1	Support
No Finding	0.963	0.999	0.959	0.979	3643
Mass	0.973	0.746	0.819	0.781	237
Suspicious Calcification	0.991	0.855	0.817	0.836	115
Asymmetries	0.978	0.356	0.203	0.258	79
Architectural Distortion	0.994	0.533	0.333	0.410	24
Suspicious Lymph Node	0.998	0.571	0.364	0.444	11
Skin Thickening	0.998	0.778	0.583	0.667	12
Retractions	0.998	1.000	0.222	0.364	9

Our model achieves a weighted Accuracy of 92.49 % and a weighted F1 score of 0.9542

Evaluated Image



Predictions

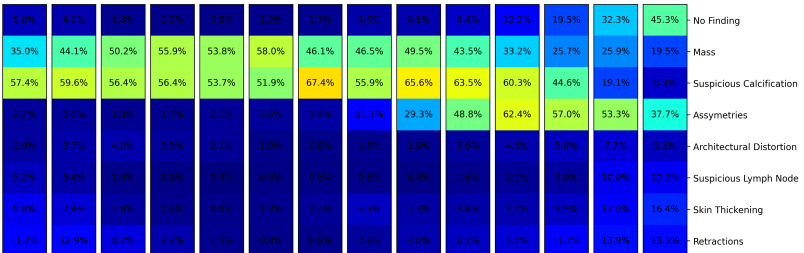
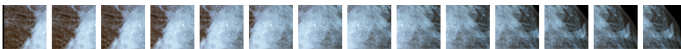


Figure: Image with bounding boxes of its findings and prediction of a row of local windows using our classifier.

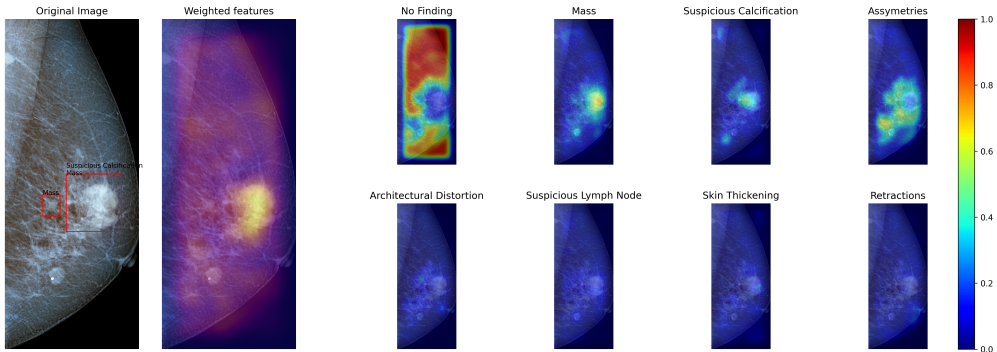
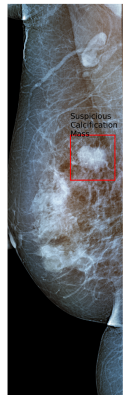
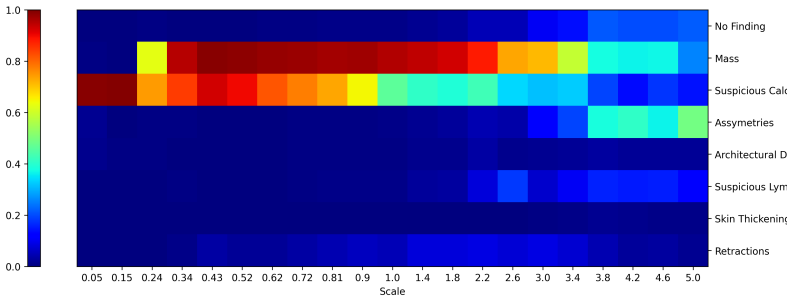


Figure: Cropped test image with bounding boxes of its findings, feature activation heatmap, and prediction of the classifier.

Image with bounding box



Predictions at defined scales



Crops at scales

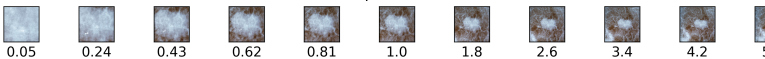


Figure: Prediction of classifier, using finding at different scales.

- Low availability of data for some classes impact performance on certain findings.
- High sensitivity of our model to less frequent findings. (e.g. Asimetries)
- Our model is able to identify findings regardless of scale of windows.

- Study of unknown-to-model images for measurement of performance with local population.

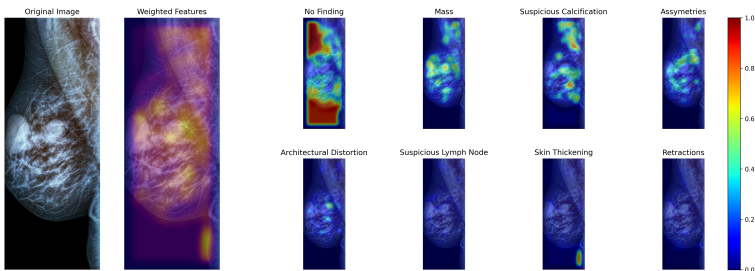


Figure: Right MLO image of Chilean patient

- Analysis of selected features and their relationship with findings, in order to identify possible biases and discard of low-performance predictions.

- [1] *Breast Cancer Statistics | World Cancer Research Fund International.* WCRF International. URL: <https://www.wcrf.org/cancer-trends/breast-cancer-statistics/> (visited on 11/09/2023).
- [2] César del SM Castillo, M. Elena C. Cabrera, Lea Derio P., et al. "Resultados Del Tratamiento Del Cáncer de Mama, Programa Nacional de Cáncer Del Adulto". In: *Revista médica de Chile* 145.12 (Dec. 2017), pp. 1507–1513. ISSN: 0034-9887. DOI: 10.4067/s0034-98872017001201507. URL: https://scielo.conicyt.cl/scielo.php?script=sci_abstract&pid=S0034-98872017001201507&lng=es&nrm=iso&tlang=en (visited on 04/21/2021).
- [3] O. Díaz, A. Rodríguez-Ruiz, A. Gubern-Mérida, et al. "¿Son los sistemas de inteligencia artificial una herramienta útil para los programas de cribado de cáncer de mama?" In: *Radiología* 63.3 (May 2021), pp. 236–244. ISSN: 00338338. DOI: 10.1016/j.rx.2020.11.006. URL: <https://linkinghub.elsevier.com/retrieve/pii/S0033833820301752> (visited on 03/30/2023).
- [4] Mehmet Gunhan Ertosun and Daniel L. Rubin. "Probabilistic Visual Search for Masses within Mammography Images Using Deep Learning". In: *2015 IEEE International Conference on Bioinformatics and Biomedicine (BIBM)*. 2015 IEEE International Conference on Bioinformatics and Biomedicine (BIBM). Washington, DC, USA: IEEE, Nov. 2015, pp. 1310–1315. ISBN: 978-1-4673-6799-8. DOI: 10.1109/BIBM.2015.7359868. URL: <http://ieeexplore.ieee.org/document/7359868/> (visited on 11/09/2023).
- [5] Steven J. Frank. "A Deep Learning Architecture with an Object-Detection Algorithm and a Convolutional Neural Network for Breast Mass Detection and Visualization". In: *Healthcare Analytics* 3 (Nov. 1, 2023), p. 100186. ISSN: 2772-4425. DOI: 10.1016/j.health.2023.100186. URL: <https://www.sciencedirect.com/science/article/pii/S2772442523000539> (visited on 11/09/2023).
- [6] Kaiming He, Xiangyu Zhang, Shaoqing Ren, et al. *Deep Residual Learning for Image Recognition*. Dec. 10, 2015. DOI: 10.48550/arXiv.1512.03385. arXiv: 1512.03385 [cs]. URL: <http://arxiv.org/abs/1512.03385> (visited on 11/10/2023). preprint.

- [7] Andrew G. Howard, Menglong Zhu, Bo Chen, et al. *MobileNets: Efficient Convolutional Neural Networks for Mobile Vision Applications*. Apr. 16, 2017. doi: 10.48550/arXiv.1704.04861. arXiv: 1704.04861 [cs]. URL: <http://arxiv.org/abs/1704.04861> (visited on 11/10/2023). preprint.
- [8] Gao Huang, Zhuang Liu, Laurens van der Maaten, et al. *Densely Connected Convolutional Networks*. Jan. 28, 2018. doi: 10.48550/arXiv.1608.06993. arXiv: 1608.06993 [cs]. URL: <http://arxiv.org/abs/1608.06993> (visited on 11/10/2023). preprint.
- [9] Ze Liu, Yutong Lin, Yue Cao, et al. *Swin Transformer: Hierarchical Vision Transformer Using Shifted Windows*. Aug. 17, 2021. doi: 10.48550/arXiv.2103.14030. arXiv: 2103.14030 [cs]. URL: <http://arxiv.org/abs/2103.14030> (visited on 11/10/2023). preprint.
- [10] Ministerio de Salud. *Informe de Vigilancia de Cáncer. Análisis de Mortalidad Prematura y AVPP Por Cáncer. Década 2009-2018*. Chile: Departamento de Epidemiología, 2021. URL: <https://www.minsal.cl/wp-content/uploads/2022/01/Informe-Mortalidad-Prematura-y-AVPP-por-C%C3%A1ncer-2009-2018.pdf> (visited on 11/09/2023).
- [11] Hieu Huy Pham, Hieu Nguyen Trung, and Ha Quy Nguyen. *VinDr-Mammo: A Large-Scale Benchmark Dataset for Computer-Aided Detection and Diagnosis in Full-Field Digital Mammography*. Version 1.0.0. PhysioNet. doi: 10.13026/BR2V-7517. URL: <https://physionet.org/content/vindr-mammo/1.0.0/> (visited on 11/08/2022).
- [12] S.M. Pizer, R.E. Johnston, J.P. Erickson, et al. "Contrast-Limited Adaptive Histogram Equalization: Speed and Effectiveness". In: [1990] *Proceedings of the First Conference on Visualization in Biomedical Computing*. [1990] Proceedings of the First Conference on Visualization in Biomedical Computing. May 1990, pp. 337–345. doi: 10.1109/VBC.1990.109340. URL: <https://ieeexplore.ieee.org/document/109340> (visited on 10/03/2023).
- [13] Alejandro Rodríguez-Ruiz, Elizabeth Krupinski, Jan-Jurre Mordang, et al. "Detection of Breast Cancer with Mammography: Effect of an Artificial Intelligence Support System". In: *Radiology* 290.2 (Nov. 20, 2018), pp. 305–314. ISSN: 0033-8419. doi: 10.1148/radiol.2018181371. URL: <https://pubs.rsna.org/doi/10.1148/radiol.2018181371> (visited on 05/12/2021).

- [14] Karen Simonyan and Andrew Zisserman. *Very Deep Convolutional Networks for Large-Scale Image Recognition*. Version 6. Apr. 10, 2015. doi: 10.48550/arXiv.1409.1556. arXiv: 1409.1556 [cs]. URL: <http://arxiv.org/abs/1409.1556> (visited on 11/10/2023). preprint.
- [15] Mingxing Tan and Quoc V. Le. *EfficientNetV2: Smaller Models and Faster Training*. June 23, 2021. arXiv: 2104.00298 [cs]. URL: <http://arxiv.org/abs/2104.00298> (visited on 11/09/2023). preprint.
- [16] Darvin Yi, Rebecca Lynn Sawyer, David Cohn III, et al. *Optimizing and Visualizing Deep Learning for Benign/Malignant Classification in Breast Tumors*. May 17, 2017. arXiv: 1705.06362 [cs]. URL: <http://arxiv.org/abs/1705.06362> (visited on 11/09/2023). preprint.